32nd Congress of the International Council of the Aeronautical Sciences
September 6-10, 2021
Pudong Shangri-La, Shanghai, China

MULTI-AXIS MANEUVER SIMULATION FOR SYSTEM IDENTIFICATION OF FLEXIBLE TRANSPORT AIRCRAFT BY HIGH-FIDELITY METHODS

Markus Ritter[1], Mathias Stefan Roeser[2] & Stefan Görtz[3]

[1]DLR - Institute of Aeroelasticity, Göttingen, Germany
[2]DLR - Institute of Flight Systems, Braunschweig, Germany
[3]DLR - Institute of Aerodynamics and Flow Technology, Braunschweig, Germany

Abstract

The development, testing and production of new aircraft are associated with considerable temporal and financial risks due to the product and manufacturing complexity. In order to accelerate the introduction of innovative technologies for more economical, more environmentally friendly and safer air transport vehicles and to better control the technological risks involved, DLR's guiding concept *The Virtual Product* aims at virtualizing the design, development and manufacturing processes. The availability of high fidelity simulation tools with the capability to model multidisciplinary phenomena is a key factor in this context. High demands are put on the numerical methods and solvers as the tools must provide reliable results in a robust manner for the entire flight envelope where nonlinearities are prominent in most of the disciplines. In this paper we present an approach for the high-fidelity multi-axis maneuver simulation, the *Virtual Flight Test*, based on multidisciplinary analysis of the free-flying elastic aircraft with CFD in the time domain. The goal is to generate virtual flight test data of high accuracy to substitute time and cost consuming real flight test campaigns to identify the flight mechanic and aeroelastic characteristics of the aircraft. Wavelet-type control surface inputs with carefully selected frequency ranges and amplitudes are used to excite the aircraft. A medium-range jet transport serves as the test case for which the approaches as well as the results of two identification maneuvers are presented and discussed.

Keywords: Virtual Flight Testing, Numerical Flight Dynamics, High-Fidelity MDA, Computational Aeroelasticity

1. Motivation

1.1 Towards Simulation-based Certification

The reduction of production time and cost of future passenger transport aircraft together with the reduction of fuel burn and emissions are nowadays the most important goals in aircraft industry. As is well known, the committed costs share of the total life cycle costs reaches its largest proportion already in the conceptual and preliminary design phases. In addition, the efforts to extract deficits are increasing considerably during the first phases of the product development and production. Besides the design-, development-, and production stages, airplane certification is one of the largest cost drivers in a commercial airplane program. Verification management relies on time- and cost-intensive flight and ground tests which of course require that the aircraft exists. A future goal for improvement is to rely on the increased application of physics based, high fidelity simulation methods as early in the design as possible to reduce costs and the time to commercial release [1]. Such approaches promise a thorough digitalization of the aircraft including its systems and the corresponding manufacturing processes and make an important step towards *simulation-based certification*. Several aerospace research institutions have already presented approaches for multidisciplinary analysis and optimization with sophisticated and computationally demanding design methods and tools [2, 3, 4, 5, 6, 7, 8, 9, 10, 11].

For the certification process, system identification flight test campaigns in which a number of dedicated maneuvers are performed are indispensable to date. From the flight test data, the aeroelastic, performance, and flight mechanic characteristics are obtained and the various simulation models used throughout the design processes can be validated and updated. The reasons that support the reduction of flight test are evident. One reason is of course trivial: in order to perform flight testing, the aircraft must exist, which means that testing takes place late. Modifications become notably expensive for the aircraft manufacturer at late stages of the development process. Due to these reasons, attempts are being made to replace the real by virtual flight tests.

The method for the virtual flight test presented in this work is based on coupling of aerodynamics, flight dynamics, and structural dynamics in space and time. The desired high accuracy necessitates an appropriate aerodynamic method. Nonlinearities such as shocks in the transonic regime as well as viscous effects in boundary layers and regions of flow separation must be considered. CFD methods based on the solution of the URANS equations on a volume grid are adequate. The fluid volume is discretized and thus the real aircraft geometry is resembled much more accurately as compared with the lifting surface approach of low-fidelity aerodynamic methods such as the VLM or the DLM. Geometrical features like flap track fairing, belly fairing, pylon, and engine cowling are represented in the CFD grid easily. The drawback of high fidelity simulations based on CFD aerodynamics is clearly the computational cost. Unsteady simulations in the time domain are required and the volume mesh must be deformed in each time step to consider structural deformations and the deflections of control surfaces. Such simulations require HPC clusters with sophisticated frameworks that support massively-parallel multidisciplinary simulations.

The foundations for the complete digital development and description of aircraft by sophisticated disciplinary and multidisciplinary simulation methods are being laid by DLR in several internal and joint research projects. The collaborative research project *VicToria* (Virtual Aircraft Technology Integration Platform) takes advantage of improved methods for the physical and numerical modeling, enhanced experimental methods, verification and validation with dedicated flight and wind-tunnel tests, and high-fidelity multidisciplinary simulation and optimization of aircraft and helicopters on high-performance computers. Virtual and real flight tests are conducted to create a virtual aircraft model for DLR's A320 research aircraft *ATRA* (Advanced Technology Research Aircraft). VicToria is a follow up to DLR's successful Digital-X project [3], where the first steps were taken towards virtual aircraft design and flight testing based on high-fidelity methods.

1.2 The Virtual Aircraft Model

The virtual flight test itself is embedded in a comprehensive process which includes the *Flying the Equations* (FTE) and the *Flying through the Database* (FTD) models. Goal of the virtual flight test is the generation of the FTE model by high fidelity multidisciplinary maneuver simulations. The data of the FTE model (e.g., the results of particular maneuver simulations with dedicated control surface input signals) is then fed into a process that generates the FTD model based on system identification algorithms. The FTD model can be seen as a reduced order model and is the preferred model for a basic nonlinear and linearized description of the flight dynamics of the aircraft. It serves, for instance, for the design of MLA and GLA systems. The described process is illustrated at a glance in Fig. 1.

The real flight test to identify the flight mechanic stability and control characteristics of the aircraft typically uses multistep, one-surface-at-time inputs for different flight conditions to excite the aircraft in its expected flight mechanic eigenmodes. Inputs such as doublets, *1-3-2-1-1* and sinusoidal signals (mostly with increasing amplitude) are comparatively easy to execute manually by experienced pilots and are therefore used as the basis for classical system identification maneuvers [12, 10]. An initial aerodynamic and flight mechanic model of the aircraft is used for the design of the input signals; the models are typically derived from wind tunnel testing or low- and mid-fidelity aerodynamic analysis. Because of uncertainties in the initial aircraft models, frequencies in a certain range above and below the expected eigenfrequencies of the flight mechanic modes must be considered for the maneuver design. Frequency sweeps are an alternative type of input for system identification. It is possible to obtain a complete frequency response of the system to a single control surface input from a single flight test point. However, each control surface must be excited separately and the length of the excitation might become comparatively long (up to 2 minutes) which renders this approach costly.

Maneuvers in which multiple control surfaces are excited simultaneously offer the potential for significant reduction of the flight test time and costs. A new kind of multi-axis input signals based on the wavelet transform has been designed and applied to system identification by Roeser [12]. The signals

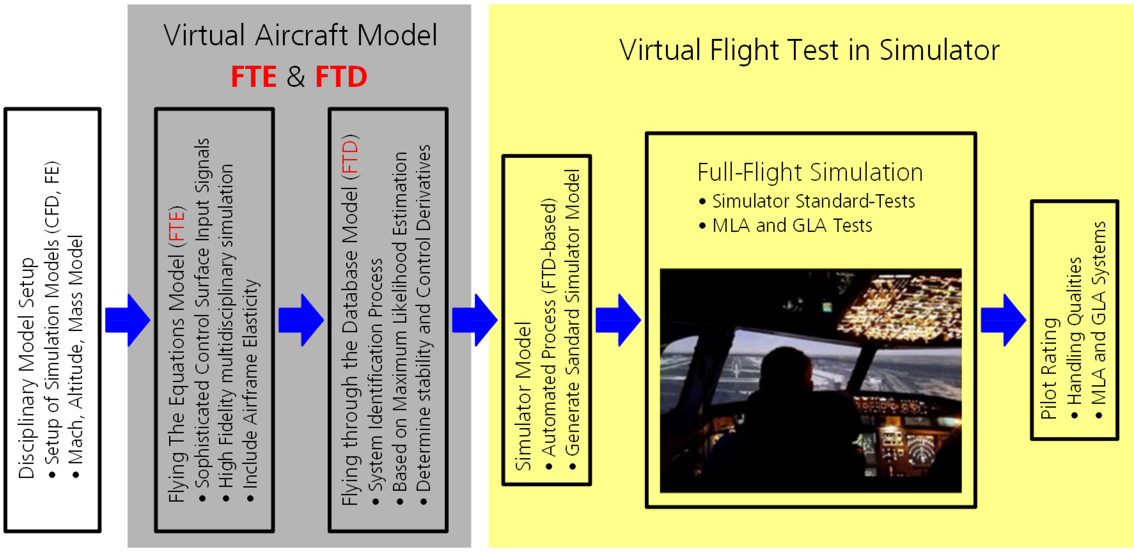

Figure 1 – Process for the derivation and integration of a Virtual Aircraft Model defined by the *FTE* and *FTD* models. The virtual flight test described in this work corresponds to the FTE model.

are parametrized by their frequency contents and the times at which the particular frequencies are excited. The wavelet transform yields a *Time-Frequency Representation* (TFR) of a signal; the signal can be uniquely reconstructed from its TFR. However, the development of such signals is an involved task. The frequency content must be chosen carefully, especially if frequency proximity of rigid-body and elastic degrees of freedom (e.g., short period mode and low frequency wing bending) emerge, which is often the case for large jet transport aircraft. Of course such complex multi-axis inputs can only be used in numerical simulations and not in real flight tests if the excitation is done by a pilot. For this work, input signals of this type are used to excite primary control surfaces – ailerons, elevators, horizontal tail plane, and rudder – of the aircraft during an unsteady multidisciplinary maneuver based on URANS aerodynamics in the time domain. No time-dependent variation of the thrust is considered since only small variations of the flight speed compared to the trim speed are expected during the maneuver. Due to the high computational costs of the time domain CFD simulation, a particular goal for the development of the multi-axis wavelet inputs is to reduce the simulation time as much as possible. The length of the multi-axis inputs used for this work is ten seconds. Wavelet-type multi-axis signals are plotted in Fig. 2, these inputs are also used for a virtual flight test in section 3.

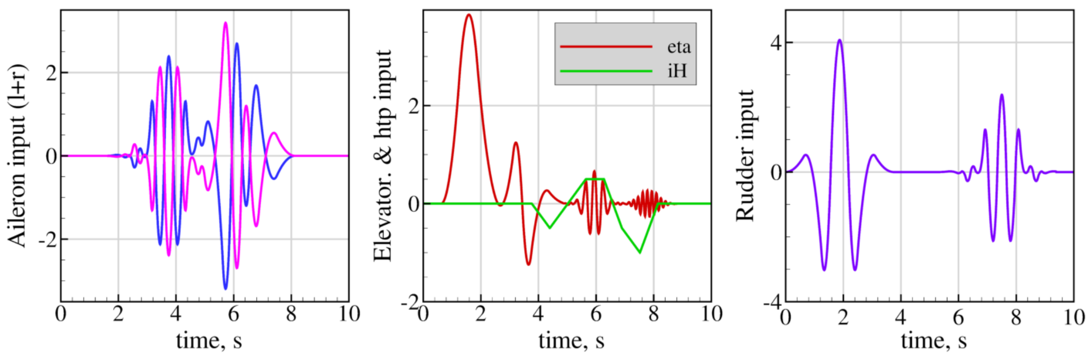

Figure 2 – Exemplary wavelet-type input signals for multi-axis actuation of primary control surfaces for the virtual flight test.

2. Numerical Models for the CFD-based Virtual Flight Test

The virtual flight test corresponds to a multidisciplinary numerical simulation for which aerodynamics, flight mechanics, and structural dynamics are coupled in space and time [3, 6, 13, 14, 10]. The aircraft is in free-flight and the flexibility of the airframe is taken into account. A steady trim simulation is performed before the actual unsteady maneuver simulation in order to obtain equilibrium of loads to ensure a steady straight level flight if no control surface inputs were applied. The unsteady maneuver simulation is then performed in discrete time domain with prescribed control surface inputs; the coupled governing equations of motion (including rigid-body and elastic degrees of freedom) and are solved for each time step. Aerodynamic forces are calculated by the CFD solver, also in discrete time steps and with moving meshes (ALE-formulation) to account for the rigid-body and the elastic motion of the aircraft.

2.1 Equations of Motion of the Free-flying Flexible Aircraft

The flight dynamics equations of motion (EOMs) for the free-flying flexible aircraft used for this work form an integral set of equations with rigid-body and elastic degrees of freedom (DOF) as independent variables. The EOMs can be derived from different mechanical principles, general derivations based on Lagrange's equations of the second kind are presented in literature [15, 16, 17, 18]. If no assumptions and simplifications are made regarding the inertial coupling between rigid-body and elastic DOFs by particular choices for the location of the body-fixed frame of reference, inertial coupling manifests between the rigid-body and the elastic DOFs by inertia and gyroscopic loads [17, 19]. A simplified flight dynamics description is obtained by using *mean axes* conditions to decouple rigid-body and elastic DOFs [18, 16]. This simplification, which is usually used together with linear methods for the calculation of structural deflections (modal approach) is justified if comparatively low structural deflections are expected (in the order of a few percent tip displacement with respect to semi-span). The test case of this work is a mid-range jet transport aircraft for which the mentioned features apply such that the governing equations based on the mean axes assumptions are used. A lumped mass model of the structure with discrete masses is used and elastic structural deformations are calculated by means of a modal approach in generalized coordinates.

The motion of the aircraft in space is described with respect to a geodetic, earth-fixed frame, and a body-fixed frame, both depicted in Fig. 3a. A set of Euler angles is used to define the attitude of the

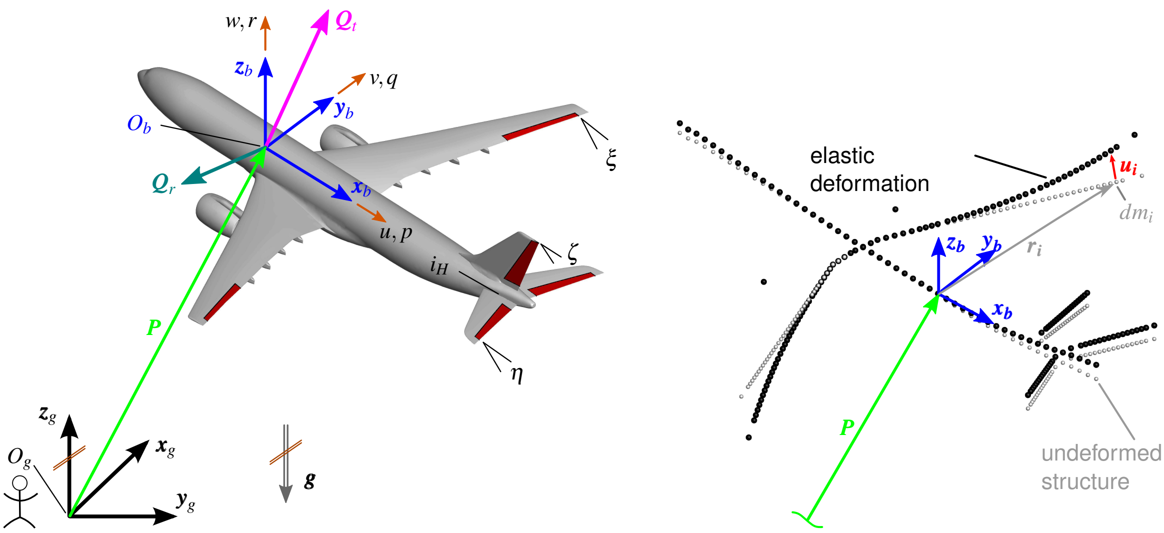

(a) Inertial (geodetic) and body-fixed coordinate frames. Body frame is fixed to the undeformed body.

(b) Lumped mass model of the airframe with discrete mass point dm_i in undeformed position, r_i, and displacement due to structural deformation, u_i.

body frame within the geodetic frame [20], angular rates of the body frame resolved in the body frame are denoted by vector $\boldsymbol{\Omega}_b$, and the velocity components along the particular axes of the body-fixed frame are denoted as $\boldsymbol{V}_b$,

$$\underline{\boldsymbol{\Phi}} = [\Phi\, \Theta\, \Psi]^T \;;\; \boldsymbol{\Omega}_b = [p\, q\, r]^T \;;\; \boldsymbol{V}_b = [u\, v\, w]^T \,. \tag{1}$$

The structural model of the aircraft is depicted in Fig. 3b, where the discrete mass elements of the lumped mass model are denoted by dm_i. The nodal displacement $\boldsymbol{u}_i$ and its velocity, $\dot{\boldsymbol{u}}_i$, of a mass point dm_i due to structural deformation (cf. Fig. 3b) are calculated by the modal approach using a superposition of the eigenvectors of the structure, ${}^{p}\boldsymbol{\Phi}^{i}$:

$$\boldsymbol{u}_i = {}^{p}\boldsymbol{\Phi}^{i}\, q_p \ ; \ \dot{\boldsymbol{u}}_i = {}^{p}\boldsymbol{\Phi}^{i}\, \dot{q}_p \ , \ (p = 1, \ldots, m) \ . \tag{2}$$

With the index m denoting the number of eigenvectors. The vector equations of motion used for the virtual flight tests in this work comprise the translational and rotational rigid-body motion as well as the elastic structural deformations [15, 16, 17, 18].
The linear momentum equation of motion is given as

$$\mathring{\boldsymbol{V}}_b\, m + \mathring{\boldsymbol{\Omega}}_b \times \overline{\boldsymbol{rm}} + \boldsymbol{\Omega}_b \times \left[\boldsymbol{V}_b\, m + \boldsymbol{\Omega}_b \times \overline{\boldsymbol{rm}} \right] - \left(\boldsymbol{M}_{bg} \boldsymbol{g} \right) m = \boldsymbol{Q}_t \ . \tag{3}$$

A ring above a variable denotes a temporal derivative with respect to the body-fixed frame of reference. The term $\overline{\boldsymbol{rm}}$ considers the inertial coupling between rotational and translational momentum, it becomes zero if the origin of the body-fixed frame is located at the center of mass of the undeformed structure. The entire mass of the aircraft is denoted by m and $\boldsymbol{g}$ denotes the gravity vector which is resolved in the geodetic frame.
The rotational momentum equation of motion is given as:

$$\boldsymbol{J} \mathring{\boldsymbol{\Omega}}_b - \mathring{\boldsymbol{V}}_b \times \overline{\boldsymbol{rm}} + \boldsymbol{V}_b \times \left[\boldsymbol{\Omega}_b \times \overline{\boldsymbol{rm}} \right] + \boldsymbol{\Omega}_b \times \left[\boldsymbol{J} \boldsymbol{\Omega}_b - \boldsymbol{V}_b \times \overline{\boldsymbol{rm}} \right] = \boldsymbol{Q}_r \ , \tag{4}$$

where $\boldsymbol{J}$ denotes the tensor of inertia of the undeformed structure. In general, the tensor of inertia can be expressed as function of the structural deformations, but it is kept constant in this work for simplicity.
Assuming a linear structural model, the governing equation of the elastic deformation for mode p is given as

$$M_{pk}\, \ddot{q}_k + \Omega^k\, q_k = Q^p \ , \tag{5}$$

where M_{pk} denotes entry (p,k) of the generalized mass matrix (for mass normalized eigenvectors, the generalized mass matrix reduces to the identity matrix), and Ω^k the eigenvalue (generalized stiffness) of the k-th structural eigenvector. To simplify the numerical integration, the hybrid (first and second order in time) EOMs presented above are formulated as a system of coupled, nonlinear ordinary differential equations (ODEs) [19].
The nonconservative generalized forces and moments for translational and rotational momentum as well as for the structural work are denoted as $\boldsymbol{Q}_t$, $\boldsymbol{Q}_r$, and Q^p, respectively. In this work, the generalized forces of the translational and angular momentum are composed of aerodynamic and propulsive (thrust) forces and moments only:

$$\boldsymbol{Q}_t = \boldsymbol{R}^A + \boldsymbol{F} \ , \tag{6a}$$

$$\boldsymbol{Q}_r = \boldsymbol{Q}^A + \boldsymbol{Q}^F \ . \tag{6b}$$

Here, $\boldsymbol{R}^A$ denotes the resulting aerodynamic forces acting on the aircraft with respect to the axes of the body-fixed frame, and $\boldsymbol{F}$ denotes the resulting propulsive forces, also resolved in the body-fixed frame. Accordingly, $\boldsymbol{Q}^A$ are the resulting aerodynamic moments, and $\boldsymbol{Q}^F$ denotes the propulsive moments, both resolved in the body-fixed frame. The generalized forces of the structural governing equation are calculated by:

$$Q^p = {}^{p}\boldsymbol{\Phi}_0{}^{T} \boldsymbol{f}^s \ , \tag{7}$$

where $\boldsymbol{f}^s$ denotes the aerodynamic forces transferred to the structural nodes. The aerodynamic forces are calculated by the CFD solver from the pressure distribution and provided at the nodes of the CFD grid (vertex-centered integration); to obtain equivalent forces on the structural nodes, a linear mapping based on an interpolation matrix is used for the (globally conservative) force transfer. The interpolation matrix is based on the evaluation of either two- or three-dimensional *radial basis functions* (RBF), where a variety of suitable RBFs can be applied, for example ones with local or global support [21, 22].

2.2 Aerodynamic Model

As mentioned in the introduction, a crucial part of the multidisciplinary analysis is the method used for the calculation of the aerodynamic forces. To obtain highly accurate results, as few assumptions and simplifications as possible are made regarding the fluid dynamics equations to be solved and the modeling of the geometry of the aircraft. Thus methods based on the solution of the potential equations (such as VLM or DLM) are not considered but a CFD method based on the solution of the RANS and URANS equations is applied. For this work, the CFD solver TAU of the DLR, which is a collection of modules for the solution of the compressible Euler and Navier-Stokes equations, is employed. Complex geometries can be modeled by hybrid, unstructured grids and several turbulence models are available together with multigrid algorithms to accelerate convergence. An ALE formulation enables time-domain solutions with moving meshes for concurrent rigid-body and elastic motions. The code is developed by DLR and validated extensively [23, 24]. For the virtual flight tests presented in this work, the TAU code is used in the RANS (for steady trim) and URANS (for unsteady maneuver) mode with the Spalart-Allmaras turbulence model.

The DLR TAU code offers an interface, the *Motion Module*, to prescribe translational and rotational rigid-body motions of the body-fixed frame of reference (which is fixed to the CFD grid). For the translational rigid-body motion, the three components of the position and velocity vector resolved along the axes of the geodetic frame of reference must be specified. For the rotational motion, the attitude (Euler angles) $\underline{\mathbf{\Phi}}$ and the body rates $\mathbf{\Omega}_b$ as defined in Eq.(1) are specified. Both translational and rotational rigid-body motions are converted to equivalent velocities of the CFD grid nodes by the Motion Module. Additionally, elastic structural deformations and velocities, $\boldsymbol{u}_i$ and $\dot{\boldsymbol{u}}_i$, as defined in Eq.(2), must be considered. The structural velocities are calculated from past grid node locations via a second-order accurate backward difference scheme.

The test cases of this work are two virtual flight tests of a mid-range jet transport aircraft. An aerodynamic and a structural simulation model represent the aircraft. The aerodynamic model consists of the CFD grid with approximately 8.5 million nodes and 25 million cells. A stack of near-wall cells with proper spacing according to the expected Reynolds and Mach numbers are used to resolve the viscous boundary layer. Flap track fairings and wingtips are modeled accurately, the outer shape and the CFD surface grid are based on surfaces derived from a high quality CAD model of the aircraft. A particular problem with CFD simulations of jet transport aircraft is the modeling of engines and nacelles. For simplicity, often through-flow nacelles are used (as has been done in previous works of the authors [6, 7, 10]). Aerodynamic influences, for example on the flow field of the main wing, are modeled acceptably by this approach; however, the resulting drag forces are of course not meaningful. A significant improvement is the use of engine boundary conditions in the CFD simulation for which the static pressure at the inlet (Fan) disk and the differences in the total pressure and total temperature are prescribed at the outlet disk, respectively. Thrust is generated by the total pressure difference and available as an "aerodynamic force" (static pressure distribution integrated over the in- and outlet boundaries of the engines). A map of the engine is required that relates the aerodynamic and thermodynamic parameters at the engine boundary disks to the thrust of the engine as function of altitude and Mach number. This method was used for the simulations presented in section 3. The high static pressure at the outlet of the engine can be seen in the bottom plot of Fig. 4.

Accurate deflections of primary control surfaces (elevator, ailerons, rudder) in CFD simulations are a complex task and object of current research. Sophisticated approaches based on Chimera and sliding or patched grid technologies are currently developed [7]. A simplified method is to apply the mesh deformation capabilities originally used for elastic structural deformations for the deflection of control surfaces. Therefore, all CFD nodes of the control surface are rotated about a prescribed hinge line and a blending region at the left and right end of the control surface allows for a smooth transition. Although simple, this method yields reliable and robust results and is used for the time-dependent deflection of the primary control surfaces (ailerons, elevators, and rudder) in the virtual flight tests. The horizontal tail plane is rotated as a whole for the trim and during the maneuver, a sliding approach based on a no-normal movement of the CFD grid nodes of the fuselage adjacent to the horizontal tail plane ensures a valid grid without negative cells.

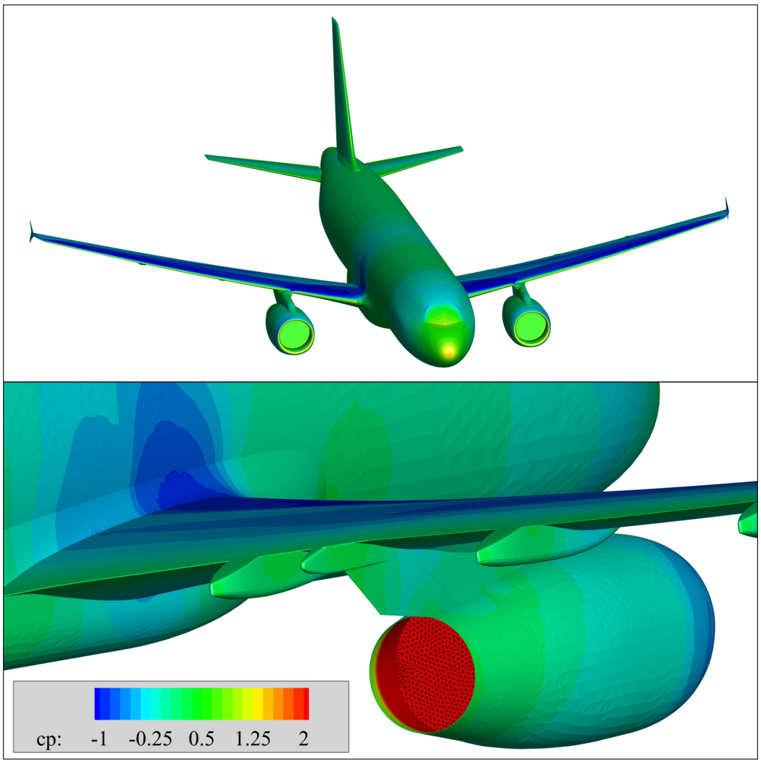

Figure 4 – Trim simulation of the jet transport with engine thrust modeled by engine boundary condition in the CFD solver.

3. Applications: Multi-Axis Maneuver for System Identification and Virtual Flight Vibration Test

Two selected applications of the high fidelity MDA approach for virtual flight testing are presented in this section. First, a multi-axis maneuver with time dependent inputs of the primary control surfaces elevator, aileron, rudder, and the horizontal tail plane. Second, a flight vibration test for which the ailerons are deflected symmetrically by a chirp signal.

3.1 Multi-Axis Maneuver for System Identification

A multi-axis system identification maneuver of 10 seconds with inputs for the horizontal tail plane, the elevator, the ailerons, and the rudder is presented first. The unsteady maneuver simulation requires initial conditions which are obtained from a trim simulation that iteratively solves for force and moment equilibrium corresponding to a steady straight level flight. The thrust required to balance the drag forces is modeled directly in the aerodynamic (CFD) model by engine boundary conditions. Based on a table for the particular engine and the airspeed as well as the altitude, the static pressure at the inlet and the total pressure and temperature difference at the outlet are prescribed for the desired thrust setting calculated by the trim solver. The pitch angle, the angle of the horizontal tail plane, the thrust of the engines, and the structural deformations are obtained from the trim procedure. For the unsteady simulations, the timestepsize of the coupled simulation is 0.005 s and the flight dynamics equations of motion are integrated in time by a semi-implicit ODE solver. The settings for the engine boundary conditions used to model thrust forces are kept constant during the entire maneuver, but unsteady inputs for the control surfaces are prescribed for each time step. Control surface inputs and results of the multi-axis maneuver are plotted in Fig. 5. This simulation was additionally performed with a rigid aircraft (with the structural deflections of the trim simulation frozen) for the same initial conditions. The wavelets are apparent in the control surface inputs [12]. The input of the elevator is characterized by four different frequencies with varying amplitudes, the reaction of the aircraft to this input is pronounced in the pitch rate, where even the highest frequencies (from approximately seven to eight and a half seconds) can be recognized. Although the aileron input starts at two and a half seconds, a rolling motion of the aircraft evolves much earlier due to the rudder input,

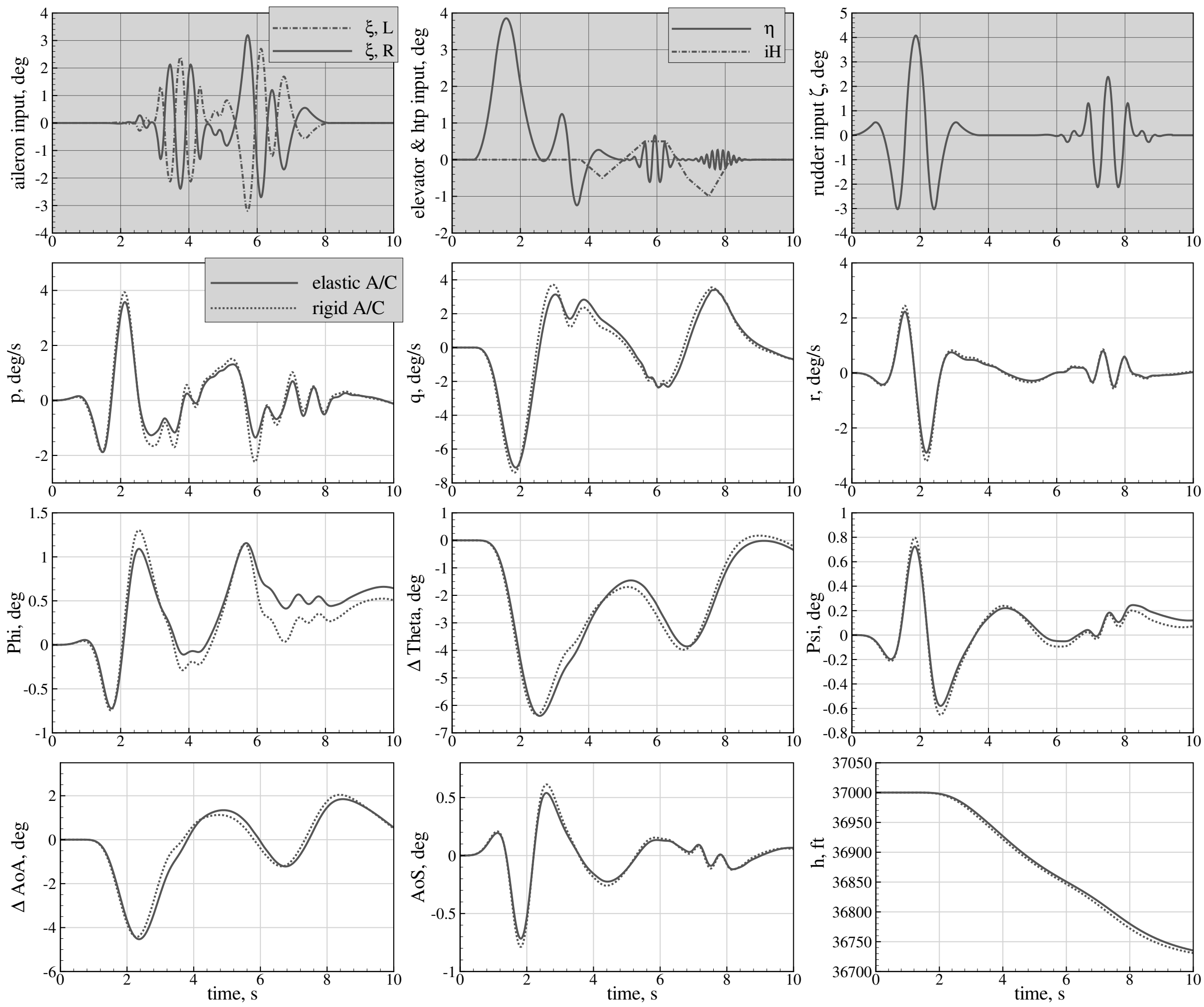

Figure 5 – Virtual flight test of multi-axis maneuver: Inputs for ailerons, elevator, horizontal tail plane (iH), and rudder; responses of elastic (solid lines) and rigid aircraft (dashed lines).

which has a strong impact on both the yawing and the rolling motion. Differences between the responses of the elastic and the rigid aircraft are distinct in all states, mostly the amplitudes of the roll, pitch, and yaw rates of the elastic aircraft are reduced compared to the rigid aircraft. The elastic structural deformation slightly dampens the peaks of the rigid-body motions. Those results – together with various other flight mechanic state vectors and the generalized coordinates – are used for the subsequent system identification process.

3.2 Virtual Flight Vibration Test

The second maneuver is a virtual flight vibration test. The "real" flight vibration test is conducted by aircraft manufacturers to identify the aeroelastic damping of the airframe experimentally as function of the airspeed at particular altitudes. The airspeed is typically increased towards the dive speed and the aircraft is excited by time dependent deflections of particular control surfaces (mostly the ailerons are used) directly from the flight control system. The length of one single maneuver can take up to several minutes, where the frequency of the excitation signal is monotonously increased up to a meaningful value, which depends on the performance of the actuator system. As such a maneuver is of high relevance for aircraft certification, it is desirable to perform it as early in the design process as possible. Using the time-domain, high fidelity MDA approach, this maneuver can be simulated as soon as all necessary simulation models are available in the design process. The key advantage of the MDA approach is that the aerodynamic nonlinearities that appear in the transonic regime during this maneuver are accounted for by the CFD method.

The numerical simulation of this maneuver was performed using the same aerodynamic, structural, and coupling model and the same trim results as for the multi-axis maneuver presented above. The input consists of a symmetric (left and right) enforced aileron excitation by a symmetric chirp signal with frequencies between 0 and 6 Hz and an amplitude of 1 degree. The aileron input signal (ξ) and the results of the simulation (selected rigid-body states as well as tip displacement and twist) are plotted in Fig. 6. As before, the thrust calculated by the trim routine is kept constant during the maneuver. As can be seen from the simulation results, the frequencies and amplitudes of the

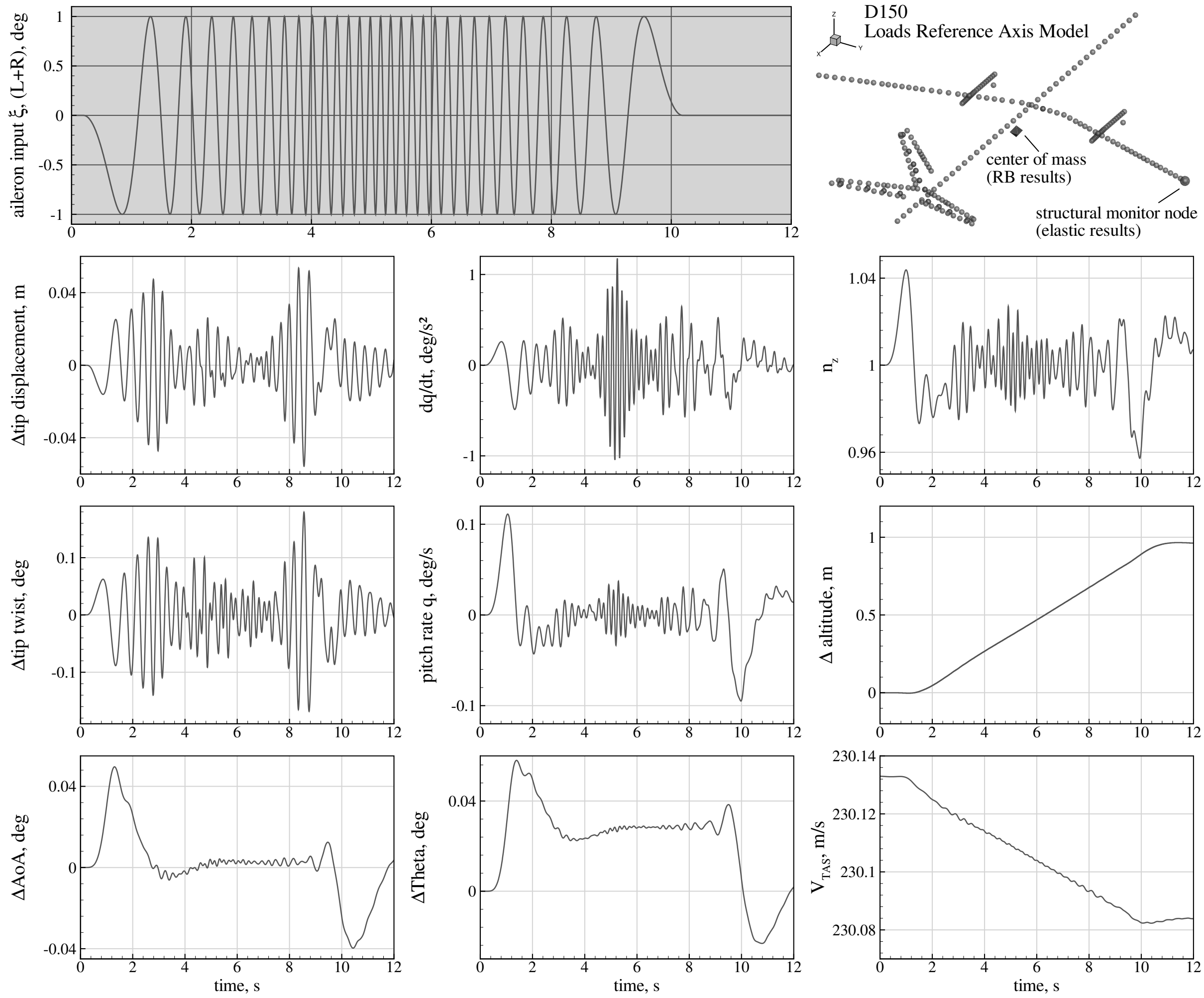

Figure 6 – Virtual flight vibration test: Symmetric inputs for ailerons; response of the elastic aircraft at center of mass as well as displacement and twist of the wing tip.

rigid-body response and the elastic structural deflections (bending and twist at the wingtip) vary significantly compared to the aileron input signal. The low-frequency structural modes massively dominate the reaction of the aircraft. Aeroelastic damping characteristics of the airframe can be calculated from the time histories of the responses. An advantage of this maneuver is that the elastic deflections are significantly more pronounced than rigid-body reactions (compared to the multi-axis maneuver above) due to the higher frequencies of the excitation signal.

4. Summary and Outlook

In order to reduce time and cost in the design and certification of aircraft, DLR is actively pursuing the ambitious long-term goal of *Certification by Simulation*. In this work, an approach for the high fidelity multidisciplinary flight dynamics simulation (Virtual Flight Test) of the free-flying flexible aircraft is presented. A volume grid based CFD method that solves the URANS equations is coupled in space and time with a nonlinear flight mechanics and a modal-based structural model. Control surface deflections are modeled by a simple but effective CFD grid deformation approach. Initial data for

the unsteady maneuver simulations in the time domain are obtained from a steady, iterative trim simulation (straight and level flight). The capabilities of the MDA framework is demonstrated by two maneuvers. The first one is a multi-axis maneuver used for the identification of the aircraft's stability and control characteristics – with less distinctive structural deformations. The second one (virtual flight vibration test) is contrary, structural deflections shall be excited in a meaningful frequency range with less pronounced rigid-body motions.
The further development and the Verification & Validation of the multidisciplinary simulation environment for virtual flight testing represents a core activity in several DLR projects. To be consistent with the multidisciplinary simulation approach, V&V must be done with experimental data of real flight tests. Such data are available from dedicated test flights with DLR's Airbus A320 ATRA research aircraft which have been conducted over the past years. Also the new DLR *iSTAR* (In-flight Systems & Technology Airborne Research) aircraft, a modified Dassault Falcon 2000LX, will be the basis for the generation of in-flight experimental data to be used for the validation of multidisciplinary simulation tools [25]. Using its advanced and integrated measurement system, iSTAR will be extensively used to generate flight test data during maneuvers at the edges of its flight envelope to support the virtual flight testing activities of DLR.

5. Contact Author Email Address

For technical questions please contact markus.ritter@dlr.de

6. Copyright Statement

References

[1] Slotnick, J. and Heller, G., "Emerging Opportunities for Predictive CFD for Off-Design Commercial Airplane Flight Characteristics," *54th 3AF International Conference on Applied Aerodynamics*, 3AF, Paris, France, March 2019.

[2] Kenway, G. K. W., Kennedy, G. J., and Martins, J. R. R. A., "Aerostructural optimization of the Common Research Model configuration," *15th AIAA/ISSMO Multidisciplinary Analysis and Optimization Conference*, Atlanta, GA, June 2014.

[3] Kroll, N., Abu-Zurayk, M., Dimitrov, D., Franz, T., Führer, T., Gerhold, T., Görtz, S., Heinrich, R., Ilic, C., Jepsen, J., Jägersküpper, J., Kruse, M., Krumbein, A., Langer, S., Liu, D., Liepelt, R., Reimer, L., Ritter, M., Schwöppe, A., Scherer, J., Spiering, F., Thormann, R., Togiti, V., Vollmer, D., and Wendisch, J.-H., "DLR project Digital-X: towards virtual aircraft design and flight testing based on high-fidelity methods," *CEAS Aeronautical Journal*, Vol. 7, No. 1, Dec. 2015, pp. 3–27.

[4] Görtz, S., Ilic, C., Abu-Zurayk, M., Liepelt, R., Jepsen, J., Führer, T., Becker, R.-G., Scherer, J., Kier, T., and Siggel, M., "Collaborative Multi-Level MDO Process Development and Application to Long-Range Transport Aircraft," *ICAS 2016*, Sept. 2016.

[5] Reimer, L., Heinrich, R., and Meuer, R., "Validation of a Time-Domain TAU-Flight Dynamics Coupling Based on Store Release Scenarios," *New Results in Numerical and Experimental Fluid Mechanics IX*, Vol. 124, 2014, pp. 455–463.

[6] Reimer, L., Ritter, M., Heinrich, R., and Krüger, W., *CFD-based Gust Load Analysis for a Free-flying Flexible Passenger Aircraft in Comparison to a DLM-based Approach*, 22nd AIAA Computational Fluid Dynamics Conference, American Institute of Aeronautics and Astronautics, Dallas, Texas, Jun 2015.

[7] Reimer, L., Heinrich, R., and Ritter, M., *Progress in the Multidisciplinary Simulation Environment FlowSimulator Towards a Virtual Flight Testing Capability of Aircraft*, Jahresbericht 2018, DGLR/STAB Symposium, Darmstadt, Germany, Nov 2018.

[8] Leicht, T., Jägersküpper, J., Vollmer, D., Schwöppe, A., Hartmann, R., Fiedler, J., and Schlauch, T., "DLR-Project Digital-X - Next Generation CFD Solver 'Flucs'," *Deutscher Luft- und Raumfahrtkongress 2016*, Februar 2016.

[9] Heinrich, R., Reimer, L., Michler, A. K., Ernst, B., Ritter, M., and Neumann, J., "DLR Pilot Applications in ComFliTe," *Computational Flight Testing*, Vol. 123, 2013, pp. 235–247.

[10] Ritter, M. R., Roeser, M. S., and Reimer, L., "CFD-based Multi-Axis Maneuver Simulation for System Identification of Flexible Transport Aircraft," *AIAA SciTech Forum*, Januar 2020.

[11] Helm, S., Haupt, M., Stickan, B., and Bleecke, H., "Advancements of CFD-CSM Coupling by Means of Multi-Body Simulation," *Deutscher Luft- und Raumfahrtkongress 2015*, 2015.

[12] Roeser, M. S., *Multi-Axis Maneuver Design for Aircraft Parameter Estimation*, Deutscher Luft- und Raumfahrtkongress (DLRK), Deutsche Gesellschaft für Luft- und Raumfahrt - Lilienthal-Oberth e.V., Friedrichshafen, Germany, Sep 2018.

[13] Müller, R. and Ritter, M., "Virtual flight testing of a controller for gust load alleviation using FMI for cosimulation," *12th International Modelica Conference*, Vol. 132 of *Linköping Electronic Conference Proceedings*, Modelica Association and Linköping University Electronic Press, Mai 2017, pp. 921–928.

[14] Reimer, L., Heinrich, R., and Ritter, M. R., "Towards Higher-Precision Maneuver and Gust Loads Computations of Aircraft: Status of Related Features in the CFD-Based Multidisciplinary Simulation Environment FlowSimulator," *21st STAB/DGLR Symposium on New Results in Numerical and Experimental Fluid Mechanics*, Vol. 142, September 2019, pp. 1–11.

[15] Waszak, M. R. and Schmidt, D. K., *On the Flight Dynamics of Aeroelastic Vehicles*, Astrodynamics Conference, Fluid Dynamics and Co-located Conferences, Williamsburg, Virginia, Aug 1986.

[16] Waszak, M. R. and Schmidt, D. K., "Flight Dynamics of Aeroelastic Vehicles," *Journal of Aircraft*, Vol. 25, No. 6, Jun 1988, pp. 563–571.

[17] Meirovitch, L., "Hybrid State Equations of Motion for Flexible Bodies in Terms of Quasi-Coordinates," *Journal of Guidance, Control, and Dynamics*, Vol. 14, No. 5, Sep 1991, pp. 1008–1013.

[18] Buttrill, C., Arbuckle, P., and Zeiler, T., *Nonlinear Simulation of a Flexible Aircraft in Maneuvering Flight*, Guidance, Navigation, and Control and Co-located Conferences, American Institute of Aeronautics and Astronautics, Monterey, California, Aug 1987.

[19] Ritter, M., Jones, J., and Cesnik, C. E. S., *Free-flight Nonlinear Aeroelastic Simulations of the X-HALE UAV by an Extended Modal Approach*, International Forum on Aeroelasticity and Structural Dynamics, Como, Italy, 2017.

[20] Brockhaus, R., *Flugregelung*, Springer Berlin Heidelberg, 2013.

[21] Beckert, A., "Ein Beitrag zur Strömungs-Struktur-Kopplung für die Berechnung des aeroelastischen Gleichgewichtszustandes," 1997, DLR Institut für Aeroelastik, Forschungsbericht 97-42.

[22] ZONA Technology, *ZAERO Theoretical Manual Version 8.4*, ZONA Technology Inc., 2011.

[23] Schwamborn, D., Gerhold, T., and Heinrich, R., "The DLR Tau Code: Recent Applications in Research and Industry," *ECCOMAS CFD 2006 Conference*, 2006.

[24] Langer, S., Schwöppe, A., and Kroll, N., "The DLR Flow Solver TAU - Status and Recent Algorithmic Developments," *52nd Aerospace Sciences Meeting*, Januar 2014.

[25] DLR, "DLR ISTAR research aircraft," `https://www.dlr.de/content/en/images/2020/1/dlr-research-aircraft-istar.html`, Accessed: 2020-11-30.